Creep Mechanism of Porous MCFC Ni Anodes Strengthened by Ni_3Al

Yun-Sung Kim
Fuel Cell Development Team, Doosan Heavy Industries & Construction Co., Ltd., Daejeon, 305–348, Korea

Jun-Heok Lim
Department of Chemical Engineering, Pukyong National University, Pusan 608–739, Korea

Hai-Soo Chun
Department of Chemical and Biological Engineering, Korea University, Seoul 136–701, Korea

DOI 10.1002/aic.10630
Published online September 12, 2005 in Wiley InterScience (www.interscience.wiley.com).

Creep tests were conducted to measure the creep rates of pure Ni, Ni/7wt%Ni_3Al, and Ni/5wt%Ni_3Al/5wt%Cr anodes for MCFCs. The resulting creep rates were well modeled by a creep rate equation. During the initial stage of sintering, the creep mechanism was affected by the microstructure, and geometry referred to the macroscopic shapes of the porous anodes. For the Ni/7wt%Ni_3Al and Ni/5wt%Ni_3Al/5wt%Cr anodes, the creep rate varied nonlinearly with time, obeying a power law with an exponent of $n < 1$, in contrast to the behavior of high-density materials, which exhibit linear Nabarro-Herring or Coble creep when subjected to an applied load. Compared to the pure Ni anode, the anodes containing Ni_3Al showed considerably increased creep resistance due to the impeding of mass transport of nickel particles in the anode when it was subjected to a compressive load. Collectively, the present results suggest that Ni/7wt%Ni_3Al and Ni/5wt%Ni_3Al/5wt%Cr anodes simultaneously have high creep resistance, and thus may represent a viable alternative porous anode for use in MCFC. *AIChE J,* 52: 359–365, 2006
Keywords: creep, MCFC, anode, Ni_3Al, sintering

Introduction

The molten carbonate fuel cell (MCFC) is one of the most popular alternative methods for electric power generation, because it is a highly efficient and environmentally clean energy conversion device that directly converts chemical energy into electrical energy and has cogeneration capability due to operating at 650°C.[1]

An important problem in the implementation of MCFC is maintaining the structure of the porous anode to ensure reliable cell operation under pressurized conditions at elevated temperatures.[2,3] This problem must be resolved if MCFCs are to be commercialized.

Over the past two decades, nickel has been widely used as the anode material in MCFCs. However, pore structure of the sintered porous nickel anode without strengthening is significantly changed by compressive stress during the operation in MCFCs. This compressive stress induces creep deformation that ultimately leads to collapse of the pore structure, resulting in a decrease in the electrochemical performance of the MCFC due to the decrease in anode surface area.[4]

Although partially sintered Ni anodes dispersed Al_2O_3, Cr, or Al particles have been manufactured to improve the creep resistance of the porous anode by dispersion strengthening or solid

Correspondence concerning this article should be addressed to Y.-S. Kim at yunsung@doosanheavy.com.

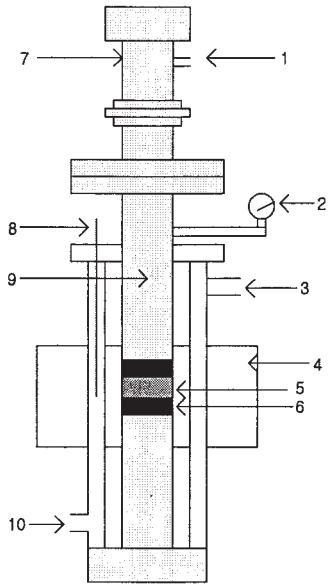

1. Air
2. Displacement indicator
3. 70%H_2/N_2 gas out
4. Furnace
5. Sample
6. Alumina plate
7. Air cylinder
8. Thermocouple
9. Pressing rod
10. 70%H_2/N_2 gas in

Figure 1. Creep test apparatus.

solution strengthening, subsequent mechanical strength in the anodes has been slightly increased due to the dispersed particles.[1]

Previously, we investigated the creep behavior and sinterability of porous anodes strengthened with Ni-Al intermetallics, especially Ni_3Al, produced by chemical synthesis in various acidic eutectic melts.[5-8]

It was also found that inclusion of particles of a second phase retarded nickel grain growth in the porous anode during sintering, and hence a stable open pore network could be maintained by controlling the amount of Ni_3Al included.[2,9-11]

To develop a more complete understanding of the strengthening of Ni anodes by including a second phase, we must consider the microstructural changes that occur during the creep deformation of the anode material. It is thought that the understanding of creep behavior in these porous materials is also of utmost importance in view of porous ceramic materials for high temperature application.

In the present study, we investigated the mechanism of creep in Ni/7wt%Ni_3Al and Ni/5wt%Ni_3Al/5wt%Cr anodes prepared to exploit the synergistic effect of dispersion strengthening and solid solution strengthening. The characteristics of these anodes were compared to those of pure Ni and Ni/10wt%Cr anodes. On the basis of our experimental results, we suggest a creep equation for these porous anodes that is different from the equation that models the behavior of high-density polycrystalline materials.

Experimental Procedures

The creep experiment was performed on samples (1×1cm) fabricated from pure Ni, Ni/7wt%Ni_3Al, Ni/5wt%Ni_3Al/5wt%Cr, and Ni/10wt%Cr anodes sintered at different temperatures to maintain the same porosity of 62%.[7,8]

The samples were first placed in the creep test apparatus, as shown in Figure 1. Then, to estimate creep activation energy in these anodes, the sample was heated at a heating rate of 100K/hr over the temperature range 723~923K. The maximum temperature error in the creep experiment was ± 0.5K.

During creep testing, 70%H_2/CO_2 mixed gas was flowed through the apparatus at a rate of 100 ml/min. The external load was transmitted to the samples by a pressing rod driven by an air cylinder, and loads ranging from 344.75kP to 1379kPa were applied to the sample to calculate the creep exponent related to the nature of the creep mechanism. In a separate set of experiments, the test was terminated after times ranging from 0 to 100 hrs.

The microstructure of each anode was analyzed by SEM-EDS (Jeol JSM-5310LV, Rontec EDWIN M1) and EPMA (Jeol JXA-8600, Shimadzu EPMA-1600).

Results and Discussion

Microstructural characterization of the MCFC anodes

The results of the SEM-EDS analysis of the sintered porous Ni, Ni/7wt%Ni_3Al, and Ni/5wt%Ni_3Al/5wt%Cr anodes are shown in Figures 2, 3, and 4, respectively. It is shown that soft-agglomerated Ni_3Al intermetallic particles exist on nickel grains but not on the nickel matrix in these samples. Although chromium appeared in all the Ni matrix and Ni_3Al by forming Cr solid solution in the Ni/5wt%Ni_3Al/5wt%Cr anode, the Cr remains as an unreacted powder (part A) due to its insufficient mass transport process during sintering at low temperature, as shown in Figure 4. In addition, the Ni/10wt%Cr anode must be

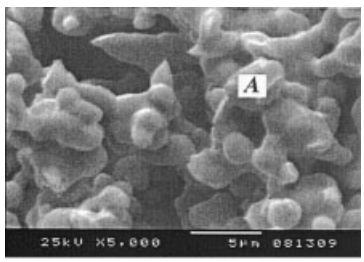

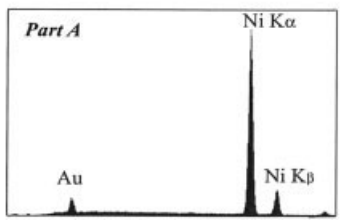

Figure 2. SEM-EDS images of pure Ni anode sintered at 873 K for 1 h.

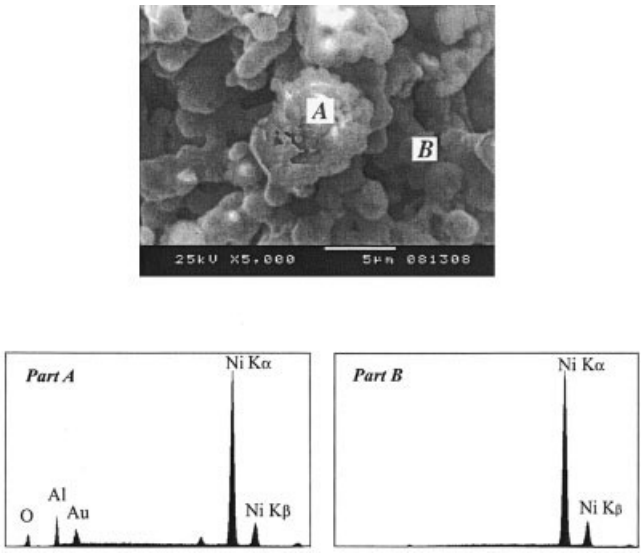

Figure 3. SEM-EDS images of Ni/7wt%Ni_3Al anode sintered at 1173 K for 1 h.

sintered at high temperature of over 1000°C to obtain the effect of solid solution strengthening by Cr addition.

It has been proposed that sintering resistance of the porous anodes for MCFCs can be increased considerably by retarding grain boundary movement, which is reinforced due to Ni_3Al dispersed through the nickel matrix at lower sintering temperature.[7-9]

Creep mechanism in the porous MCFC anodes

Creep is the plastic deformation proceeding at constant stress or at constant load and constant temperature in time. When a crystalline solid is subjected to a static external load, individual atoms adjust their positions in such a way that the equilibrium between external forces and interatomic force is maintained. Macroscopically, this adjustment of atomic positions manifests as a deformation. The deformation leads to displacements which, if large enough, can be measured macroscopically.

At homologous temperatures higher than about 0.4, grain boundaries represented a system of glide planes, which generally becomes active simultaneously with crystallographic glide systems within the grains. The homologous temperature is defined as the ratio T/T_m, where T is the temperature under consideration and T_m is the melting temperature of the material.

Thus, under the action of applied stress, grain boundary sliding occurs and this contributes to the plastic strain. In the temperature regime where grain boundary sliding occurs, the sliding phenomenon causes extreme heterogeneity of the plastic deformation. This can lead to reduction in the polycrystal compatibility by formation of voids on grain boundaries if the grain boundary sliding is not accommodated by diffusion of vacancies, i.e., due to diffusion creep. Diffusional creep, which also contributes to the plastic strain, can occur by diffusion of vacancies either within the crystal lattice (Nabarro-Herring creep) or via grain boundaries (Coble creep).

In general, the steady state creep rate equation for high-density polycrystalline materials is a function of temperature and applied stress. In the case of diffusional creep in high-density materials, such as pure metals, the creep equation is represented by the following equation

$$\dot{\varepsilon} = \frac{ADGb}{kT}\left[\frac{b}{G}\right]^p\left[\frac{\sigma}{S}\right]^n = \frac{AD_oGb}{kT}\left[\frac{b}{G}\right]^p\left[\frac{\sigma}{S}\right]^n \exp\left[-\frac{Q}{RT}\right] \tag{1}$$

where the diffusion coefficient, D, is defined by the usual expression $D = D_o\exp(-Q/RT)$ and Q is the creep activation energy of creep. At constant temperature and applied stress, the creep mechanism can be examined by obtaining the values of p, n, and Q from Eq. 1. Diffusional creep can occur by diffusion of vacancies either via the Nabarro-Hearing creep or via the Coble creep, and the creep rate under these creep mechanism is dependent on the applied stress, with $n = 1$.

On the other hand, the dependence of the creep rate of porous materials on the applied stress, compressive or tensile, is usually expressed by the following general equation

$$\dot{\varepsilon} = f(G, \rho, T)\sigma_o^n \tag{2}$$

where $f(G,\rho,T)$ is a complicated function of the powder geometry (G), microstructure (represented by the relative density, ρ), and temperature (T), and the exponent, n, is related to the nature of the creep mechanism. Accordingly, the creep exponent in Eq. 1 can be determined by comparing creep results for samples with the same density, temperature, and geometry, obtained under different applied stresses. If the creep phenomenon is substantially amenable to a Nabarro-Hearing creep or Coble creep, n should be equal to 1, while $n > 1$ would indicate a behavior in the plastic range.[12-15]

Considering the relative density of a porous anode for MCFC, its creep rate equation can be written as follows

$$\dot{\varepsilon} = A\sigma^n\exp\left[-\frac{Q}{RT}\right]\exp[-B\rho] \tag{3}$$

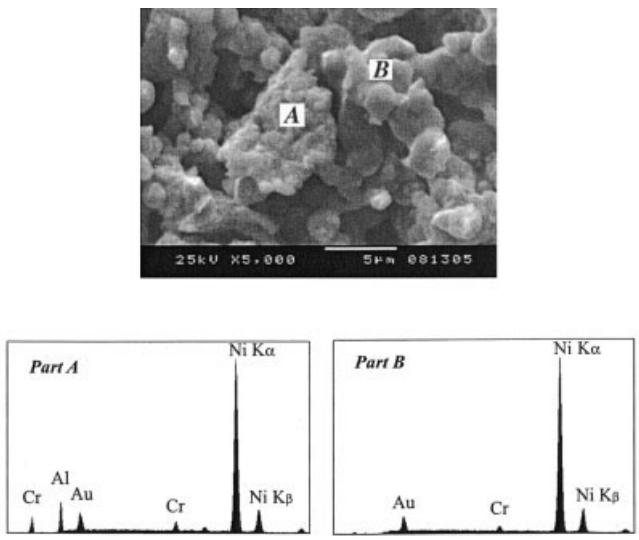

Figure 4. SEM-EDS images of Ni/5wt%Ni_3Al/5wt%Cr anode sintered at 1173 K for 1 h.

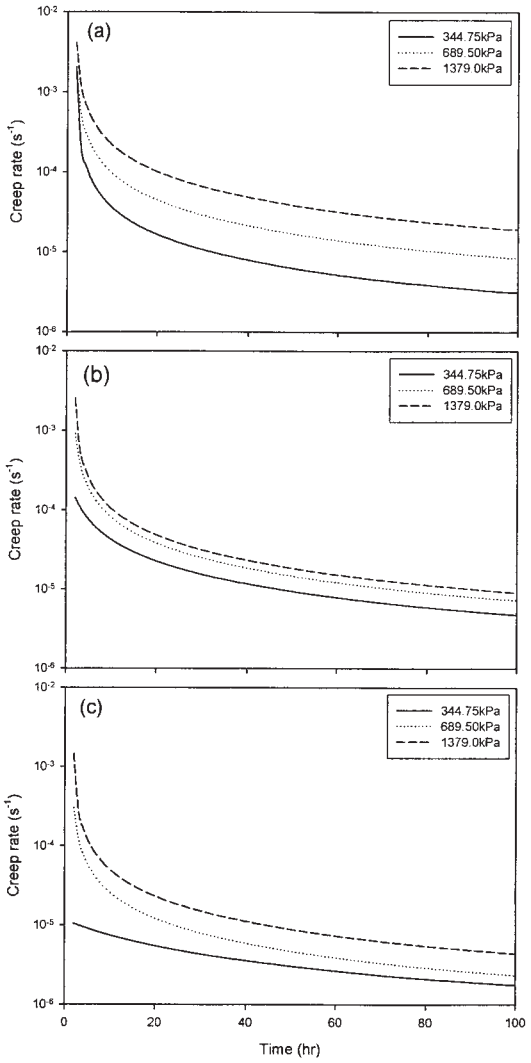

Figure 5. Creep rate curves for (a) pure Ni, (b) Ni/7wt%Ni_3Al, and (c) Ni/5wt%Ni_3Al/5wt%Cr anodes under different applied loads at 923 K.

where A is a fitting parameter and B is a resistance coefficient that represents resistance against creep deformation. In this equation, the term dependent on the powder geometry of the anode is expressed simply by the relative density, which represents the ratio of solid density to total density, when porosity of the anode is considerably high.

Effects of applied load on the creep rate of the various porous anodes at 923K are shown in Figure 5. For all anodes, the creep rate decreases with increasing test time.

Previous studies of creep strain in porous anodes have shown that the creep behavior in these porous anodes consisted of two stages of the creep curve, which is different from those of high-density polycrystalline materials.[7,8] Therefore, it is seen that the creep rate of the Ni/5wt%Ni_3Al/5wt%Cr anode is considerably lower than those of the others, and then the creep behaviors are stabilized quickly to the second stage. Initially, the creep rates of the Ni/7wt%Ni_3Al and Ni/5wt%Ni_3Al/5wt%Cr anodes decrease rapidly with increasing applied stress, in contrast to the behavior observed for the pure Ni anode. It is reasonable to assume that the dominant creep mechanism of these anodes should be attributed to instability of particle-to-particle contacts, as the creep behaviors in the initial creep region are influenced considerably by the applied stress.

Actually, as shown in previous study of morphological changes during the creep test, these porous anodes, during the initial stage of sintering, seem to undergo grain boundary connections. This process is probably due to the inherent instability of solid/pore systems,[16,17] which is certainly enhanced in systems with very high porosity.

The creep exponent, n, can be obtained from plots of the logarithm of the creep rate against the applied stress at a fixed creep time. The results are shown in Figure 6 and yield a family of nearly parallel straight lines. Deviation from average slopes of the anodes is observed only for relatively short creep times ranging from 2 to 8 hrs, probably in the transition to the second stage of the creep regime. The transition from the first to the second creep regime is consistent with a rearrangement of the nickel particles in the porous structure to more stable sites

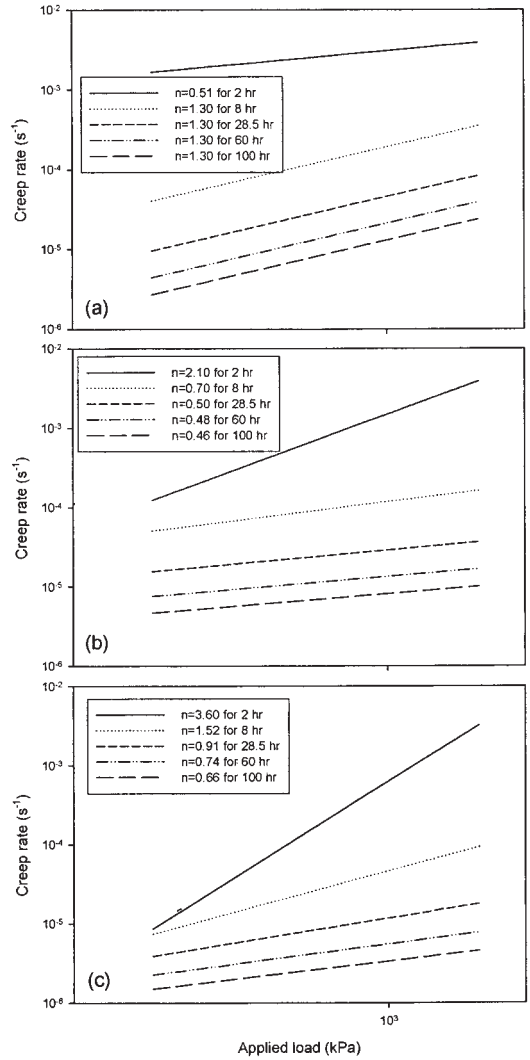

Figure 6. Creep exponents of (a) pure Ni, (b) Ni/7wt%Ni_3Al, and (c) Ni/5wt%Ni_3Al/5wt%Cr anodes at 923 K.

Table 1. Parameters of the Creep Model Eq. 3 Obtained from the Creep Test

Anodes	n [−]	Q [kJ mol^{-1}]	A [Mpa^{-n} s]	B [−]
Pure Ni	1.30	24.18	2.64×10^2	21
Ni/7 wt% Ni_3Al	0.54	41.15	9.63×10^{17}	98
Ni/5 wt% Ni_3Al/5 wt% Cr	0.96	38.06	4.85×10^{14}	85

induced by the applied stress. The evidence that the logarithm of the creep rate plots linearly against the logarithm of the applied stress proves that Eq. 2 can be applied to the present data.

The average creep exponents of pure Ni, Ni/7wt% Ni_3Al, and Ni/5wt%Ni_3Al/5wt%Cr anodes obtained from the creep test after 8 hrs are shown in Table 1. The creep exponent of the pure Ni anode is similar to that of Nabarro-Hearing or Coble creep, for which n = 1 should be expected. In the case of the Ni/7wt% Ni_3Al and Ni/5wt%Ni_3Al/5wt%Cr anodes, the creep exponents are less than 1.

The substantial constancy of the creep exponent with time suggests its weak dependence on the actual density in the experimental range. Considering that both the mean grain size and the average pore size are uniquely determined by the sample density, it should be inferred that the creep exponent is also independent of such variables. Nevertheless, a dependence of n on the microstructural shape parameters, weakly related to actual density, average pore, and grain size, cannot be excluded. If so, the creep nature of $n < 1$ should be due to a creep mechanism of particle rearrangement and packing changes. Such effects are little related to bulk properties and should be particularly active during the initial stages of sintering of the porous Ni/7wt%Ni_3Al and Ni/5wt%Ni_3Al/5wt%Cr anodes.

Figure 7 shows the effect of temperature on the creep behaviors of the anodes at fixed uniaxial load of 689.50kP. Although the creep strain of the anodes is generally increased with increasing temperature, the creep strain of Ni/5wt%Ni_3Al/

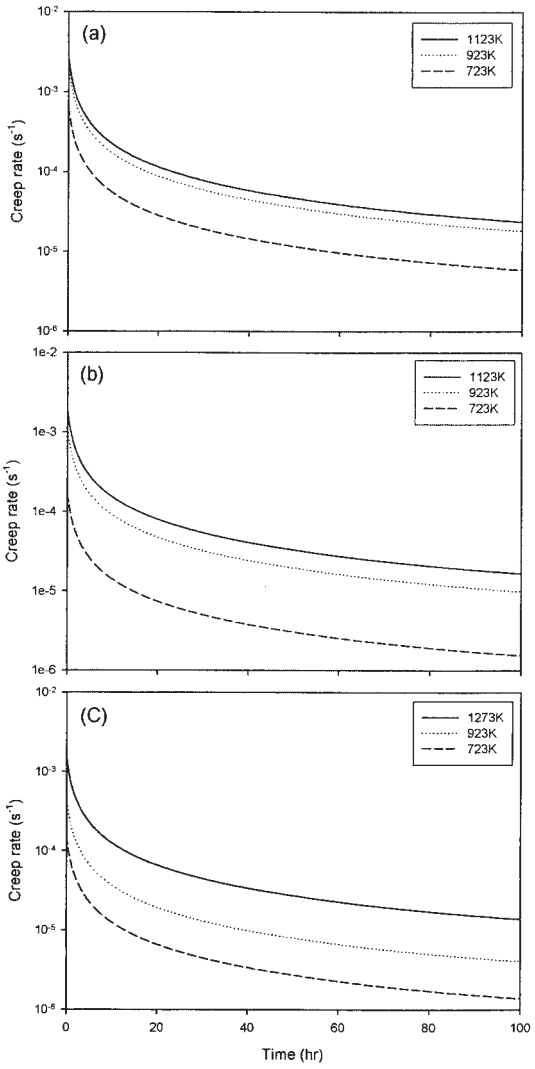

Figure 7. Creep rate curves for (a) pure Ni, (b) Ni/7wt%Ni_3Al, and (c) Ni/5wt%Ni_3Al/5wt%Cr anodes at different temperatures under 689.50 kPa.

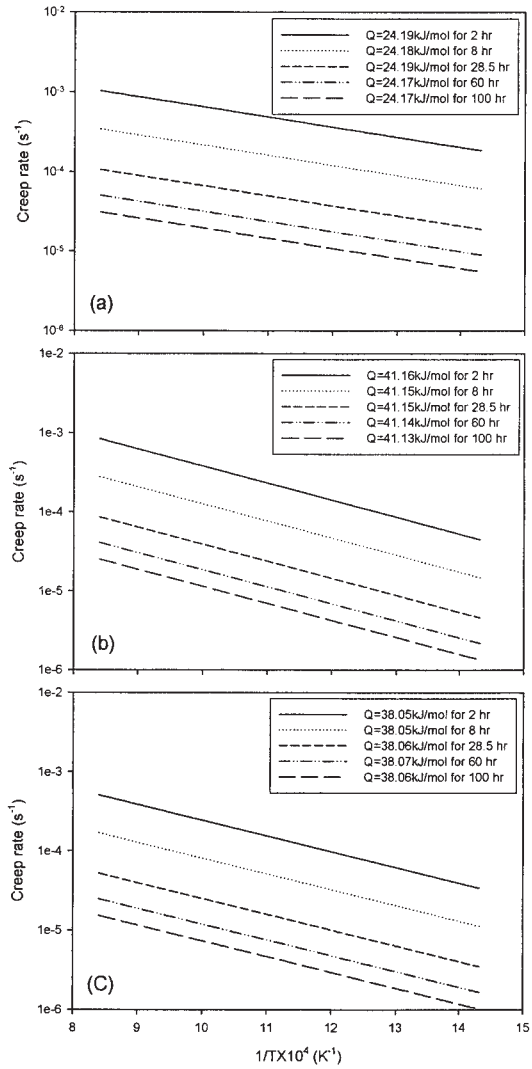

Figure 8. Creep activation energies for (a) pure Ni, (b) Ni/7wt%Ni_3Al, and (c) Ni/5wt%Ni_3Al/5wt%Cr anodes

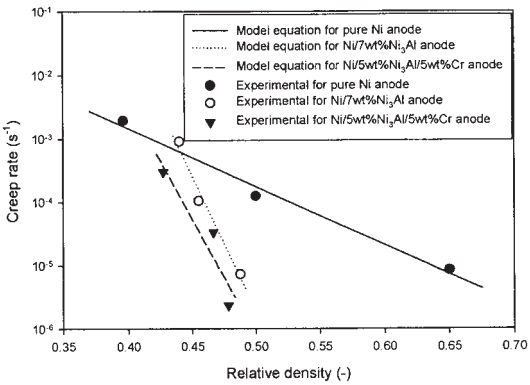

Figure 9. Effect of the relative density on the creep rate during creep test for 100 h at 923 K.

5wt%Cr anodes can be increased at 1123K at least and the creep rate of the anode is also relatively lower than other anodes. It is thought that the Ni/5wt%Ni_3Al/5wt%Cr anode can be considered as an alternative anode for MCFC, which is operated at 923K, so creep resistance of the anode is considerably effective at high temperature.

The creep activation energies for the anodes can be derived from the data in Figure 7, by plotting the logarithm of the creep rate against reciprocal temperature at fixed applied stress, as shown in Figure 8. The creep activation energies of these anodes calculated in this way are shown in Table 1. The activation energies for the Ni anodes with Ni_3Al inclusion are about 40 $\pm$ 2 kJ/mol by high creep rate gradient depending on temperature gradient. Compared with activation energy for grain boundary diffusion of Ni powder with 108 kJ/mol, the creep activation energy for the pure Ni anode is no more than 24.18 kJ/mol. It is thought that the creep activation energies for the porous anodes are smaller than those of mass transport during sintering, so pore contact geometry in the anodes is different from that in high-density materials.

Relationships between creep rate estimated from model Eq. 3 and the creep rate measured after the creep test for 100 hrs are shown in Figure 9, by plotting logarithmically the creep rate against relative density. The experimental results are consistent with the model equation used to explain the creep behavior of porous anodes. The values of the parameters A and B estimated by Eq. 3 are shown in Table 1.

The creep rate of the porous anodes is dependent on the relative density, so the logarithm of the creep rate is inversely proportional to the relative density. It is shown that the resistance coefficient of Ni/7wt%Ni_3Al and Ni/5wt%Ni_3Al/5wt%Cr anodes are higher than that of the pure Ni anode, because the slopes of the creep rates are considerably decreased with increasing density.

Conclusion

It was investigated from microstructural analysis that sintering resistance of Ni/7wt% Ni_3Al and Ni/5wt%Ni_3Al/5wt%Cr anodes can be considerably increased by retarding the nickel grain boundary movement due to Ni_3Al dispersed in the nickel matrix, and subsequently creep resistance was increased by impeding mass transport accelerated under the applied stresses.

The creep rate equation for the anodes was obtained by considering the microstructure expressed by the actual relative density, and the rate estimated by the equation was consistent with the experimental results obtained in creep tests. In the creep equation, the nature of the creep exponents for Ni/7wt%Ni_3Al and Ni/5wt%Ni_3Al/5wt%Cr anodes ranged from 0.54 to 0.96, because of creep phenomena accompanying the early stage of sintering of these anodes. For the pure Ni anode, the creep exponent was 1.3.

Also, the creep activation energies for the anodes obtained from the creep tests were lower than those of high-density materials.

Notation

A = dimensionless constant or fitting parameter (−)
B_R = resistance coefficient (−)
b = Burger's vector (unit: m)
D = diffusion coefficient (unit: m^2/s)
D_o = proportionality constant of diffusion coefficient (unit: m^2/s)
G = grain size (m)
k = Boltzmann constant (J/K)
n = creep exponent (−)
p = exponent of the inverse grain size (−)
Q = creep activation energy (kJ/mol)
R = gas constant
S = shear modulus (Pa)
T = sintering temperature (K)

Greek letters

$\dot{\varepsilon}$ = steady state creep rate (s^{-1})
ρ = relative density (−)
σ = applied stress (Pa)

Subscripts and superscripts

o = initial

Abbreviations/Acronyms

MCFC = molten carbonate fuel cell

Literature Cited

1. Yuh C, Johnsen R, Farooque M, Maru H. Status of carbonate fuel cell materials. *J Power Sources.* 1996;56(1):1-10.
2. Kim YS, Choo HS, Shin MC, Hong MZ, Lim HJ, Chun HS. Effect of Ni_3Al inclusion on pore structure in the porous anode for molten carbonate fuel cell. *Korean J Chem Eng.* 2000;17(5):497-501.
3. Lim JH. Kim YS, Choo HS, Shin MC, Lee SI, Chun HS. Effect of Ni_3Al inclusion on nickel grain growth inhibition in the porous MCFC anode. *Proc 3rd International Fuel Cell Conference.* 1999;413-416.
4. Lim JH, Yi GB, Suh GH, Lee JK, Kim YS, Chun HS. A simulation of electrochemical kinetics for gas-liquid-solid phase of MCFC anode. *Korean J Chem Eng.* 1999;16:856-860.
5. Kim YS. Chun HS. Sintering characteristics of a porous Ni/Ni_3Al anode for molten carbonate fuel cell. *J Power Sources.* 1999;84(1): 80-86.
6. Kim YS, Choo HS, Shin MC, Hong MZ, Lim JH, Chun HS. Chemical synthesis of Ni-Al intermetallics in the eutectic salt baths for a MCFC anode additive. *Proc 3rd International Fuel Cell Conference.* 1999; 417-420.
7. Kim YS, Lee KY, Chun HS. Creep behavior of a porous Ni/Ni_3Al anode for molten carbonate fuel cell. *Proc The 2000 Fuel Cell Seminar.* 2000;743-746.
8. Kim YS, Lee KY, Chun HS. Creep characteristics of the porous Ni/Ni_3Al anodes for molten carbonate fuel cells. *J Power Sources.* 2001;99(1-2):26-33.
9. Kim YS, Lee SI, Lim JH, Chun HS. Nickel grain growth inhibition with Ni_3Al intermetallics in porous MCFC anode. *J Chem Eng Jpn.* 2000;33(1):96-102.

10. Kim YS, Shin MC, Lim JH, Lee KY, Lee JK, Chun HS. Electrochemical reaction at gas-liquid-solid interface of a porous anode for molten carbonate fuel cell. *Proc 7th Asian Conference on Fluidized-Bed and Three-Phase Reactors.* 2000;527-532.
11. Kim YS, Lee SI, Lim JH, Chun HS. Effect of Ni_3Al addition on the grain growth in porous Ni/Ni_3Al anode materials for molten carbonate fuel cell. *J Chem Eng Jpn.* 2001;34(8):979-984.
12. Beruto D, Capurro M, Botter R. Thermally activated step for densification and creep of high-porosity MgO compacts in the intermediate sintering stage. *J Eur Ceram Soc.* 1999;19(5):623-628.
13. Bouvard D, McMeeking RM. Deformation of interparticle necks by diffusion-controlled creep. *J Am Ceram Soc.* 1996;79(3):666-672.
14. Cannon WR, Langdon TG. Creep of ceramics, Part 1. Mechanical characteristics. *J Mater Sci.* 1983;18(1):1-50.
15. Cannon WR, Langdon TG. Creep of ceramics, Part 2. An examination of flow mechanics. *J Mater Sci.* 1988;23(1):1-20.
16. Dole SL, Prochazka S, Doremus H. Microstructural coarsening during sintering of boron carbide. *J Am Ceram Soc.* 1989;72(6):958-966.
17. Wong B, Pask JS. Models for kinetics of solid state sintering. *J Am Ceram Soc.* 1979;62(3):138-141.

Manuscript received July 11, 2004, and revision received Jun. 17, 2005.